Prediction of underground mining-induced subsidence: Artificial neural network based approach

Long Quoc Nguyen[1, 2✉] ⓘ, Tam Thanh Thi Le[1, 3✉] ⓘ, Trong Gia Nguyen[1, 3✉] ⓘ, Dinh Trong Tran[4*✉] ⓘ

[1] *Faculty of Geomatics and Land Administration, Hanoi University of Mining and Geology, Hanoi, Vietnam*
[2] *Innovations for Sustainable and Responsible Mining, Hanoi University of Mining and Geology, Hanoi, Vietnam*
[3] *Geodesy and Environment, Hanoi University of Mining and Geology, Hanoi, Vietnam*
[4] *Department of Geodesy and Geomatics Engineering, Hanoi University of Civil Engineering, Hanoi, Vietnam*
*Corresponding author: e-mail trongtd@huce.edu.vn

Abstract

Purpose. Mining-induced land subsidence is a significant concern in areas with extensive underground mining activities. Therefore, the prediction of land subsidence is crucial for effective land management and infrastructure planning. This research applies an artificial neural network (ANN) to predict land subsidence over the Mong Duong underground coal mine in Quang Ninh, Vietnam.

Methods. In the ANN model proposed in this research, four features are used as the model inputs to predict land subsidence, i.e., model outputs. These features include the positions of ground points in the direction of the trough main cross-section, the distance from the chamber (goaf) center to the ground monitoring points, the accumulated exploitation volume of extraction space, and the measured/recorded time. The entire dataset of 12 measured epochs, covering 22 months with a 2-month repetition time period, is divided into the training set for the first 9 measured epochs and the test set for the last 3 measured epochs. *k*-fold cross-validation is first applied to the training set to determine the best model hyperparameters, which are then adopted to predict land subsidence in the test set.

Findings. The best model hyperparameters are found to be 5 hidden layers, 64 hidden nodes and 240 iterated epochs. Root Mean Square Error (RMSE) and Mean Absolute Error (MAE) of the predicted land subsidence depend on the time separated between the last measured epoch and the predicted epoch. Within 2 months from the last measurements, RMSE and MAE are at 22 and 13 mm for Epoch 10, which increase to 31 and 20 mm for Epoch 11 (4 months from the last measurement) and 37 and 24 mm for Epoch 12 (6 months from the last measurement).

Originality. A new ANN model with associated "optimal" hyperparameters to predict underground mining-induced land subsidence is proposed in this research.

Practical implications. The ANN model proposed in this research is a good and convenient tool for estimating mining-induced land subsidence, which can be applied to underground mines in Quang Ninh province, Vietnam.

Keywords: subsidence prediction, underground mine, machine learning, artificial neural network (ANN)

1. Introduction

Mining operations play a vital role in global economic growth and development. One of the benefits of mining is resource provision, which provides valuable minerals, metals, and other resources to various industrial sectors, e.g., manufacturing, construction, energy [1]. Additionally, mining provides jobs [2] not only for miners, but also for representatives of other fields, such as geological engineers, surveyors, and electricians. In Vietnam, the mining industry has a long history and has made a significant contribution to the Vietnamese economy, providing a huge number of jobs [3]. The Vietnamese ore occurrence is diverse and contains about 70 types of minerals [4], among which coal is one of the main mineral sources. Most of Vietnam's coal mines are located in the northeast province of Quang Ninh (a.k.a. Quang Ninh Coal Basin). Of these, there are about 30 underground and 20 open-pit coal mines, the exploration volume of which is projected to increase yearly. However, the proportion of underground

mines is increasing as some open-pit coal mines are converted to underground due to their increasing depth [5]. The role of Vietnamese coal is not only in economic growth in terms of mineral exports, but also in political energy security in terms of coal-fired electricity generation [6].

While mining has made contributions to the field of economics, it poses environmental, social, and public health challenges [7]. One of those environmental problems is land subsidence. The excavation of mineral resources during mining disrupts the internal stress equilibrium [8]. Consequently, the extraction of minerals from underground deposits results in the sinking or lowering of the Earth's surface, a phenomenon known as mining-induced land subsidence [9]. This occurrence presents substantial risks to infrastructure, environmental stability, and human safety in mining regions [10]. Various methods are employed to measure mining-induced land subsidence, with common methods including leveling [11], Global Navigation Satellite System

(GNSS) [12], [13], and Interferometric Synthetic Aperture Radar (InSAR) [14]-[16]. While measuring land subsidence caused by mining activities is essential after the Earth's surface has sunk, there is a growing need for efficient management and prediction of future mining-induced land subsidence. This is crucial for sustainable mining practices and land use planning [17]. Traditional subsidence prediction methods, such as the empirical approach based on a combination of experience and analysis of a large set of observations [18], and the analytical approach relying on computerized mathematical models [19], have been widely employed. However, these methods often fall short in accuracy and predictive capability. In recent years, Artificial Neural Networks (ANNs) have emerged as a promising tool for subsidence prediction, owing to their capability to capture complex nonlinear relationships within datasets [20]-[22].

This article aims to apply ANNs to predict underground mining-induced land subsidence, leveraging their strengths in pattern recognition, adaptive learning, and generalization. The study utilizes a dataset comprising the positions of ground points in the direction of the trough main cross-section, the distance from the chamber center to the ground monitoring points, the accumulated exploitation volume of extraction space, and the measured/recorded time. This dataset is used to train, validate, and predict mining-induced land subsidence using ANN models. The application of ANNs in subsidence prediction in underground mining has the potential to improve the accuracy and reliability of subsidence forecast, enabling proactive measures for land management and infrastructure planning. By investigating the capabilities of the ANN models in predicting underground mining-induced land subsidence, this study aims to contribute to the advancement of subsidence prediction techniques and support sustainable mining practices.

2. Study area, materials, and methods

2.1. Study area

This study focuses on the Mong Duong underground coal mine in the Northeast province of Quang Ninh, Vietnam (Fig. 1). Mong Duong is located within the administrative boundaries of Cam Pha City, Quang Ninh Province, approximately 10 km north of the city center. It is adjacent to the Mong Duong River and the East Sea to the north and northeast, and shares borders with the Bac Quang Loi and Bac Coc Sau coal mines to the south, and the Khe Cham coal mine to the west.

The Mong Duong coal mine is selected in this study because it is one of the oldest, established in 1982, and largest underground coal mines in Vietnam, with a capacity of 1.5 million tons per year. Moreover, Mong Duong is an ongoing mine, in which many residential houses and important infrastructures, e.g., wastewater treatment or railway systems, are located in close proximity. This makes those infrastructures susceptible to land subsidence caused by mining exploration. The selected mine is located in an area with complex geological factors associated with various tectonic activities, such as faulting and folding. The topography of the Mong Duong coal mine is characterized by low to medium mountains, with the highest point reaching 165 m in the central area.

2.2. Data

In this study, land subsidence (η) is measured using GNSS technology. At the same time, other relevant measurements were recorded, including the positions of ground points in the direction of the trough main cross-section (Y),

the distance from the chamber center to the ground monitoring points (L), the accumulated exploitation volume of extraction space (V), and the measured/recorded time (T).
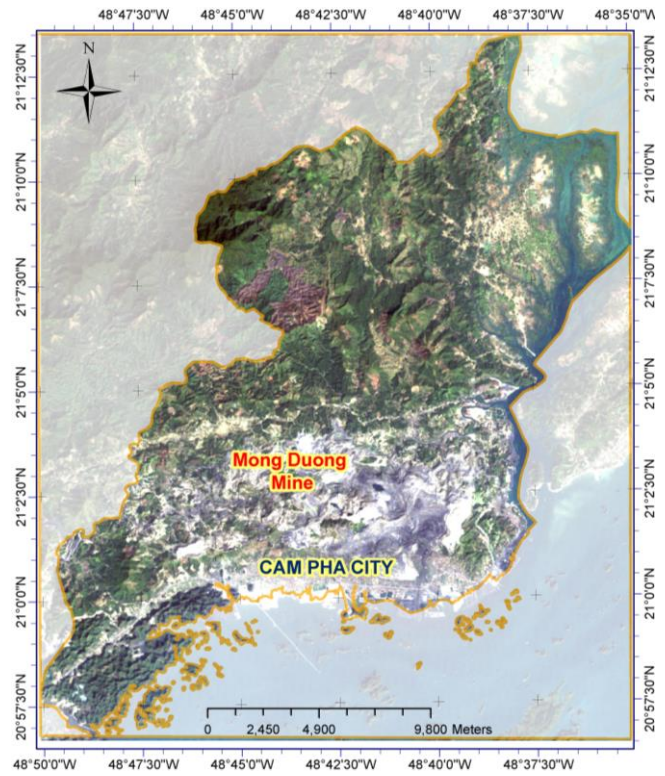

Figure 1. Study area of the Mong Duong underground coal mine

Those measurements are shown in Figure 2 as an underground mining configuration with three measurement times T_1, T_2, and T_k, corresponding to three chamber centers O_1, O_2, and O_k. There are 22 points measured at 12 epochs with a 2-month time interval. As a result, there are a total of 242 instances, each involving the above-mentioned four features (i.e., Y, L, V, and T). These instances are then used to predict land subsidence (i.e., η) using ANN.
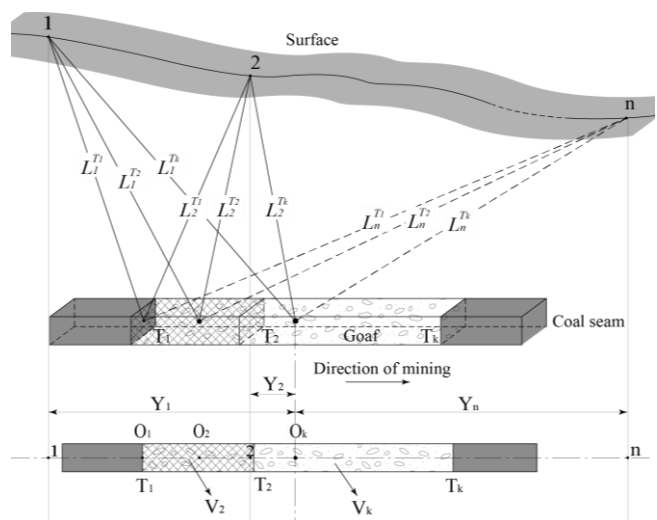

Figure 2. Underground mining configuration indicating the relationship between input variables used in this study: Y – the positions of ground points in the direction of the trough main cross-section; L – the distance from the chamber center to the ground monitoring points; V – the accumulated exploitation volume of extraction space; t – the measured/recorded time

Figure 3a shows the positions of measured points in the direction of the trough main cross-section (red dots and texts). The subsidence η has a relationship with the Y feature that, at a specific epoch, higher subsidence is observed from points situated closer to the trough center. This relationship is shown in Figure 3a with each line corresponding to a measured epoch. Figure 3a also indicates that subsidence underwent continuous change up to the final measured epoch (cf. lines corresponding to earlier and subsequent epochs). This trend is confirmed by the relationships between the measured subsidence η and the measurement time t of all points in Figure 3b. The figure shows that measured points exhibited continuous subsidence over time with different subsidence rates, depending on their locations as indicated above.

(a)

(b)
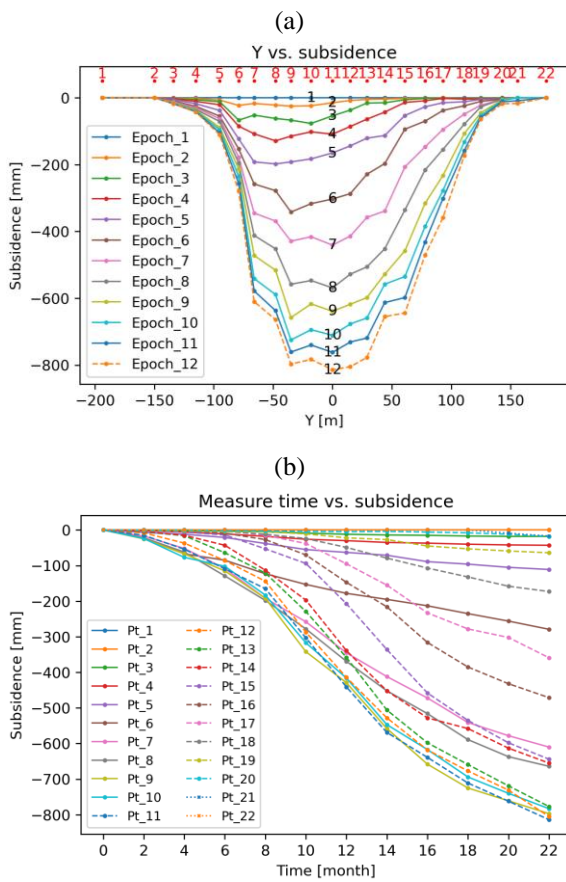
Figure 3. Relationships between measured subsidence η and input variables: (a) the distance to the trough center Y; (b) measured time; red dots and texts in (a) indicate the locations of the measured points and their corresponding indices

Given that Mong Duong is an ongoing underground mine, we expect the accumulated exploitation volume regularly increased over time. As a consequence, a relationship between land subsidence η and the V feature, similar to that with the t feature, can be found in Figure 4a that a larger accumulated exploration volume V leads to higher subsidence at all points. We note that, while the measurements were taken regularly over time, the mining exploitation concluded at cycle 7, corresponding to the 12th month. This results in the exploitation volume V remaining unchanged at 78000 m² from that cycle (Fig. 4b). However, land subsidence persisted beyond cycle 7, as shown in Figure 3. Consequently, at the same measured point, the same volume of 78000 m² yields different subsidence, as shown in Figure 4a.

(a)

(b)
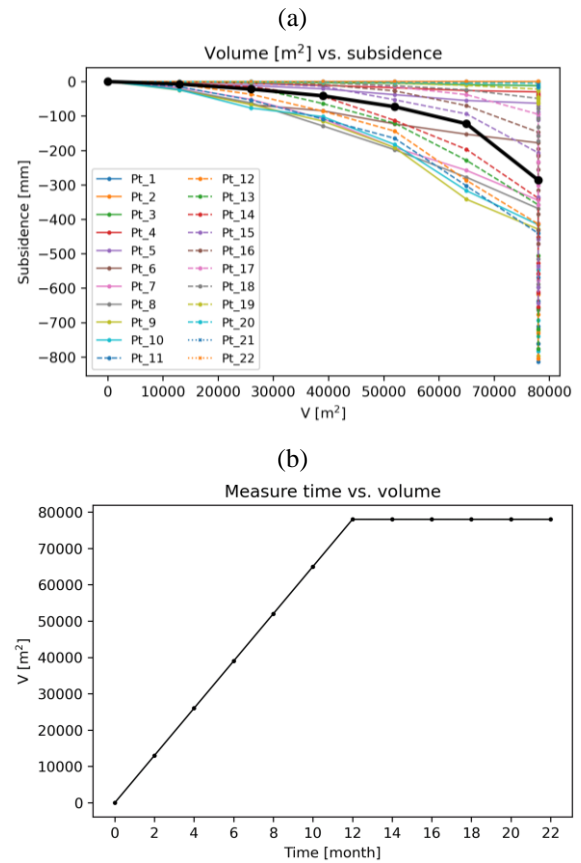
Figure 4. Relationships between measured subsidence η and input variables: (a) accumulated exploitation volume V; (b) the change of accumulated exploitation volume V over time; the solid black line in (a) corresponds to the mean subsidence computed for each volume V

The black solid line in Figure 4a shows the mean subsidence computed for each volume V, which confirms the general trend that a higher volume corresponds to a larger subsidence.

The subsidence of a point changes over time depending on the progress of mining exploitation, as depicted by the movement of the chamber (Fig. 2). This movement, in turn, leads to a change in the slope distance from the point to the chamber center. As a result, the change of L depends on the location of the measured point. More specifically, points 1-5 exhibited increases in L over time, while points 11-22 appeared to undergo decreases in L. In contrast, points 6-10 exhibited a U-shaped trend, i.e., L decreased during initial epochs before increasing during the later epochs (Fig. 5a). These trends propagate to the relationship between L and the subsidence η, as shown in Figure 5b, in which points 1-5 indicate an increase in L corresponding to an increase in land subsidence.

Conversely, an opposite trend is observed in points 11-22, in which the decrease in L corresponds to higher subsidence. A U-shape trend can be seen in points 6-10, in which the decline in L at initial epochs is followed by an increase at subsequent epochs, leading to larger subsidence at each point. Like the exploitation volume V, the distance L changed from Epoch 1 to Epoch 7 corresponding to the 12th month and remained unchanged after the cessation of mining exploitation.

2.3. Artificial Neural Networks

ANNs are among the most powerful artificial intelligence tools in land subsidence prediction owing to their capacity to learn complex patterns with large datasets, facilitating accurate predictions [20]-[23].
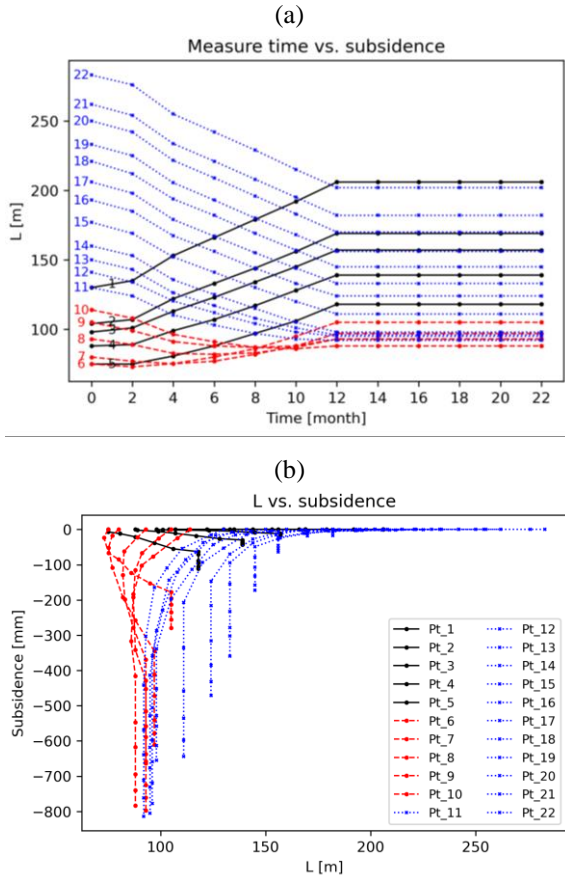
(a)

(b)

Figure 5. Changes in the slope distances from measured points to the chamber center L due to mine exploitation: (a) changes over time; (b) relationships with the measured subsidence η

ANNs are computational models inspired by the structure of the human brain, and thus neural networks [24]. These networks are composed of interconnected artificial neuron layers, which are divided into input, hidden, and output layers (Fig. 6).
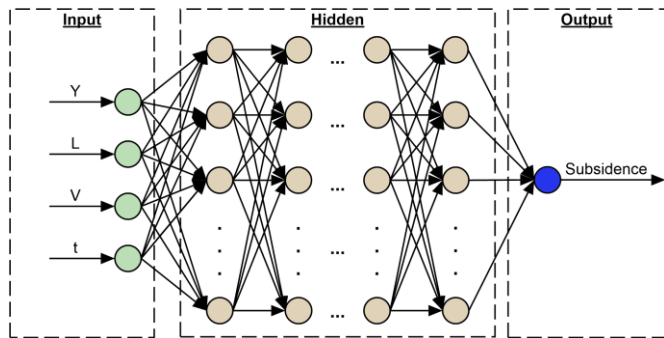

Figure 6. Structure of artificial neural network with input, hidden, and output layers; the input layer involves four nodes corresponding to four input features Y, L, V, and t; the numbers of layers and nodes in the hidden section are determined experimentally by the k-fold cross-validation; the output layer involves one node corresponding to the predicted subsidence

The input layer imports the input features and then passes them through the hidden layers, in which computations are conducted with a series of weighted connections to estimate the predicted variables in the output layer. The weights are initially assigned with random values in the input layer, which are then propagated through the hidden and output

layers. The weights are subsequently adjusted by optimization algorithms, e.g., gradient descent and backpropagation [25]. In this way, ANN can accurately predict output variables by adjusting the weights.

In an ANN, each layer involves one or more neurons depending on the particular problem being investigated. In this study, the input layer includes four neurons corresponding to four input features Y, L, V, and t as mentioned above. The hidden layer section includes one or more layers, each incorporating a number of nodes. In this study, the "optimal" numbers of hidden layers, hidden nodes, and iterated backpropagation epochs are experimentally determined by the so-called k-fold cross-validation [26].

2.4. Model performance evaluation

To evaluate the performance of mining-induced land subsidence prediction by ANN, two commonly used validation metrics are employed in this study, including Root Mean Square Error (RMSE) and Mean Absolute Error (MAE). Both RMSE and MAE measure the average magnitude of the errors, i.e., the difference between measured and predicted subsidence [27], [28]. While RMSE is sensitive to outliers because it assigns higher weights to measurements with larger errors, MAE is more robust to outliers because it is less affected by the magnitude of errors [27]. Both RMSE and MAE are used in this study because of their complementation to each other. RMSE and MAE are estimated using the equations provided below [27]:

$$RMSE = \sqrt{\frac{\sum_{i=1}^{n}(\eta_i - \hat{\eta}_i)^2}{n}} \; ; \tag{1}$$

$$MAE = \frac{\sum_{i=1}^{n}|\eta_i - \hat{\eta}_i|}{n} \, , \tag{2}$$

where:

η_i and $\hat{\eta}_i$ – the measured and predicted subsidence;

n – the number of validated measurements used to estimate RMSE and MAE.

The difference between measured and predicted subsidence $\eta_i - \hat{\eta}_i$ is prediction error Δ_i.

3. Results and discussion

In this study, we test the prediction of mining-induced surface deformation by ANN. With a total of 12 measured epochs at a 2-month interval, as shown in Section 2.2, we apply an ANN model with the first 9 epochs selected as the training set, and the remaining 3 epochs selected as the test set. This is to test the influence of the time separation between measured epochs and the interpolation time, i.e., at 2, 4, and 6 months after the last measured epoch. We apply an ANN network with the Rectified Linear Unit (ReLU) chosen as the activation function in the hidden layers [29]. ReLU is a frequently used function in both classification and regression problems due to its simplicity, requiring less computation compared to other functions, such as Sigmoid (a.k.a Logit of LogSig) [30] or Tanh [31]. With the aim of predicting surface subsidence, the regression problem is used, thereby no activation function is applied to the output layer. Instead, a weighted sum is used. Additionally, the objective of this study is to predict surface subsidence with the highest possible precision, which is usually represented by RMSE; there-

fore, Mean Squared Error (MSE) is used as the lost/cost function, and MAE is used as the metric. This function, together with the backpropagation algorithm [32], is applied to estimate the model parameters, utilizing the Root Mean Square Propagation (RMSProp) optimizer [33].

To identify the most appropriate network structure, a *k*-fold cross-validation is adopted [26]. *k*-fold cross-validation is a special case of validation in machine learning applied to small datasets. It is adopted to select the best model hyperparameters, including the numbers of hidden layers, hidden nodes, and iterated epochs. Here, a 4-fold cross-validation is applied based on the number of available instances. Specifically, 4 groups of contiguous measured epochs are selected from the 9 training set measured epochs. In each fold step, one group is held out as the validation set, while the remaining 3 groups are selected as the reduced training set. The ANN model is then trained based on this reduced training set. The model with associated parameters derived from this training step is then applied to the validation to estimate the validation RMSE/MAE. The final RMSE/MAE is then derived by averaging over the 4-fold steps. This 4-fold cross-validation is applied to all hyperparameters in sequence. In this way, the best model with associated parameters is selected if it is of the smallest validated RMSE/MAE. In each examination to select the best model hyperparameters, normalization and standardization are applied to the dataset [34].

We first examine the "optimal" number of hidden layers in the model, keeping other hyperparameters fixed. Specifically, to minimize the computation burden, a model with 16 hidden nodes (i.e., the nodes in the hidden layers) and 100 iterated epochs is utilized. This model is used to test different numbers of hidden layers, ranging from 1 to 7. The relationships between the RMSE/MAE of the training and the validation sets and the number of hidden layers are shown in Figure 7a. The results indicate that the mean RMSE/MAE of the training set (dashed lines in Figure 7a) continuously decreases until 7 hidden layers, with little improvement from 6 hidden layers onward. In contrast, the mean RMSE/MAE of the validation set (solid lines in Figure 7a) decreases from 1 to 5 hidden layers, but begins to increase from 6 hidden layers. This suggests that the model likely starts overfitting at 6 hidden layers, and that 5 hidden layers are the most appropriate for the final model structure. Figure 7a also shows that a higher number of hidden layers requires a longer mean computation time. The mean computation time increases almost linearly between 1 and 5 hidden layers, but a significant increase of about 30% at 7 hidden layers. With 5 hidden layers, the mean RMSE and the mean MAE of the training set are 18 and 12 mm, respectively, while those of the validation set are 36 and 26 mm, and the mean computation time is 1.7 seconds.

With 5 hidden layers assigned to the model, we then examine the most appropriate number of hidden nodes, i.e., the nodes in the hidden layers. Like the previous test on the number of hidden layers, to minimize the computation cost, the number of iterated epochs is fixed to 100, and the number of hidden nodes is tested as the power of two, from 2 (i.e., 2^1) to 1024 (i.e., 2^{10}). For the sake of simplicity, the same number of nodes is used in all 5 hidden layers. The results in Figure 7b indicate that 64 hidden nodes are the best in both mean RMSE and MAE of the training and validation sets.
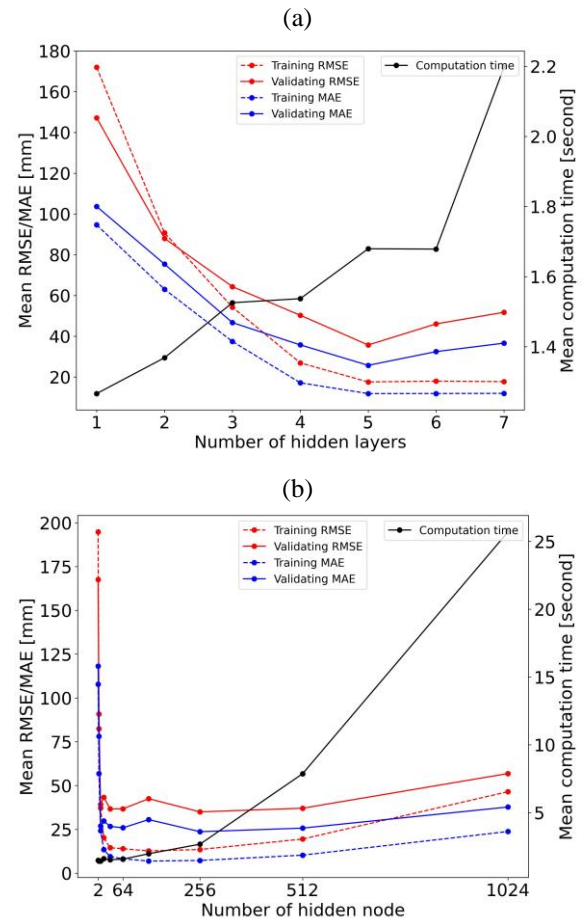

Figure 7. Relationships between the mean RMSE (red) and MAE (blue) of the training set (dashed lines) and validation set (solid lines) with the ANN model parameters in k-fold cross-validation: (a) the number of hidden layers; (b) the number of hidden nodes; black lines in both sub-figures indicate the corresponding computation time

The mean RMSE/MAE reduce significantly from 2 hidden nodes (at 172 mm and 94 mm with the training set, and 147 and 103 mm with the validation set), to 64 (2^6) hidden nodes (at 18 and 12 mm with the training set, and 46 and 32 mm with the validation set), before increasing from 128 (2^7) hidden nodes. Like the test on the number of layers, a longer computation time is required for larger numbers of hidden nodes (see the black line in Figure 7b).

We then examine the most appropriate number of iterated epochs used in the backpropagation algorithm of the ANN model. Here, the "optimal" 5 hidden layers and 64 hidden nodes are adopted, while the number of iterated epochs is changed from 1 to 1000 epochs, with the results shown in Figure 8. As the results show a fluctuation in both mean RMSE (Fig. 8a) and MAE (Fig. 8b), we apply a 10-epoch moving average to smooth the results (see blue lines in Figure 8). The results suggest that a higher number of iterated epochs leads to a lower moving average mean RMSE/MAE for both the training and validation sets, with a significant improvement observed between 1 and around 100 iterated epochs. The minimum moving average RMSE and MAE for the validation set are found at 240 iterated epochs, at 30 and 20 mm, respectively (see black dashed lines in Figure 8). The computation time exhibits a linear trend according to the change in the number of iterated epochs, with the "optimal" number of iterated epochs corresponding to a mean computation time of approximately 3.2 seconds.
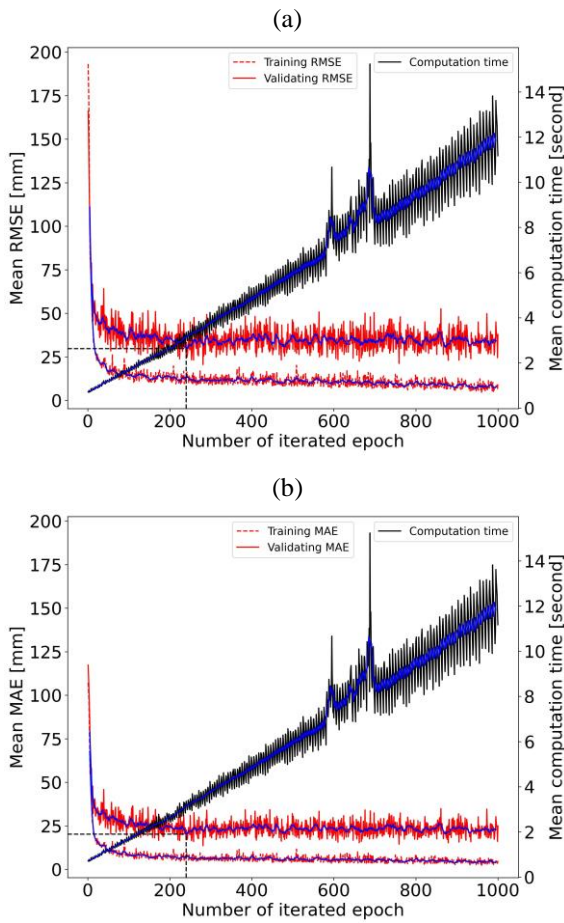
(a)

(b)

Figure 8. Relationships between model performance evaluation metrics of the training set (dashed lines) and validation set (solid lines) with the number of iterated epochs in k-fold cross-validation: (a) the mean RMSE; (b) the mean MAE; black solid lines in both subfigures indicate the corresponding computation time and blue lines indicate a 10-epoch moving average; black dashed lines indicate the best number of iterated epochs in terms of the mean RMSE/MAE of the validation set

The "optimal" hyperparameters of the ANN model have been obtained as 5 hidden layers, 64 hidden nodes, and 240 iterated epochs. These "optimal" parameters are then adopted to predict mining-induced land subsidence over the study area of the Mong Duong underground mine. As mentioned above, we predict subsidence for the last three measured Epochs 10, 11, and 12 corresponding to the 18th, 20th, and 22nd months. The predicted results for the 22 measured points are shown in Figure 9, and their performance evaluation is shown in Table 1.

Table 1. Performance evaluation of the test set (unit – mm)

Epoch	RMSE	MAE
Epoch 10	22	13
Epoch 11	31	20
Epoch 12	37	24

The good fit between the blue and orange lines in Figure 9 indicates the effectiveness of the proposed ANN model in accurate land subsidence prediction. Both the RMSE and MAE of the predicted land subsidence depend on the time separation between the last measured epoch and the predicted epoch. Within two months from the last measurement, RMSE/MAE of 22 and 13 mm are observed for Epoch 10.
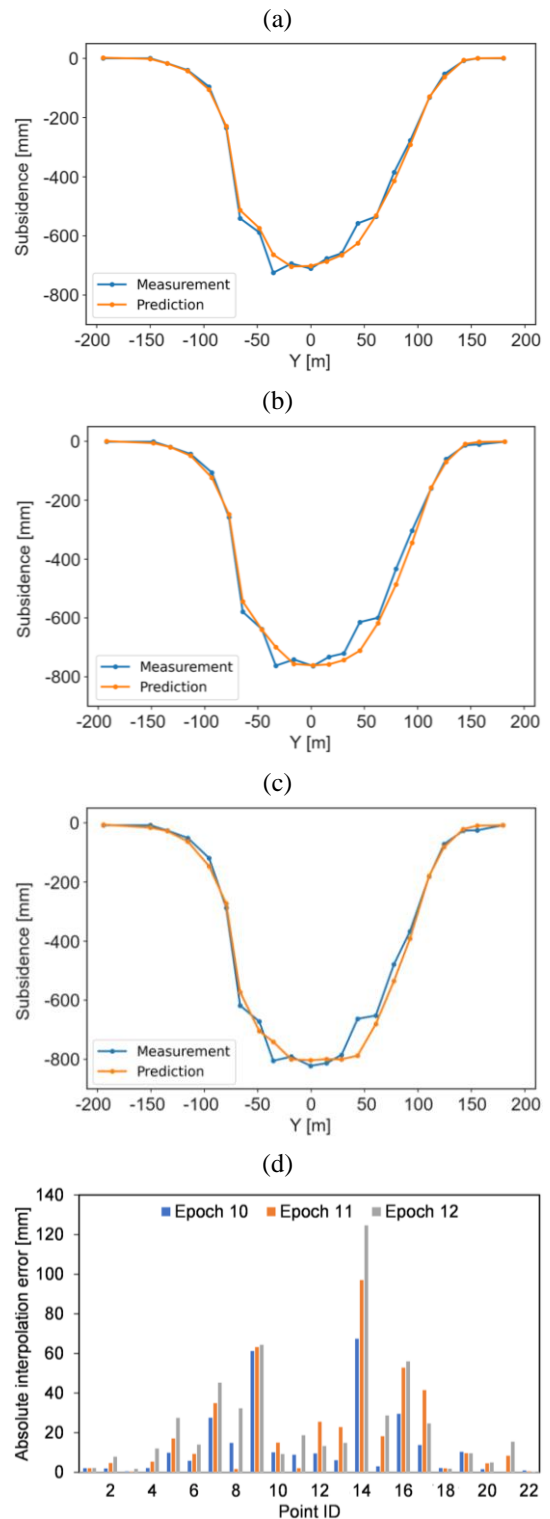
(a)

(b)

(c)

(d)

Figure 9. Mining-induced land subsidence predicted by ANN for the 22 measured points over the three test epochs: (a) Epoch 10; (b) Epoch 11; (c) Epoch 12; (d) absolute interpolation error of the 22 measured points at the three interpolation epochs

These numbers increase to 31 and 20 mm for Epoch 11 (4 months from the last measurement), and 37 and 24 mm for Epoch 12 (6 months from the last measurement) (Table 1). The dependence of the interpolation error on the time separation between the last measured epoch and the interpolation epoch is confirmed by Figure 9d, indicating the absolute interpolation error, i.e., the absolute difference between measured and predicted subsidence.

While this study has demonstrated favorable outcomes in predicting underground mining-induced subsidence using an ANN-based approach, there is a recognized need for future research aimed at refining prediction performance. The current study utilized a time series spanning 12 epochs over 22 months but given the continuous generation of extensive data from underground mining activities, incorporating more recent measurements is essential for enhanced accuracy. Furthermore, the study employed measurements in a 2D profile along the measurement line (refer to Figure 2). Expanding the measurement configuration to a 3D surface is anticipated to bolster prediction performance, capturing the movement of the entire surface rather than being limited to a single profile. To advance predictive modeling, particularly in understanding subsidence patterns, more sophisticated approaches such as deep learning can be explored. Additionally, in instances where the time series of deformation measurements (η) is available without corresponding model inputs, e.g., *L, Y, V* in this study, the model may not function effectively. In such cases, adopting a direct or recursive univariate prediction model, such as long short-term memory, which uses past subsidence as inputs to predict future subsidence, is recommended.

4. Conclusions

This study has applied ANN to predict land subsidence measured by GNSS over the Mong Duong underground coal mine, in Quang Ninh, Vietnam. There were 22 points measured with 12 epochs, which were divided into the training set for the first 9 measured epochs, and the test set for the last 3 measured epochs. Land subsidence was measured by GNSS for each epoch, together with the positions of ground points in the direction of the main trough cross-section, the distance from the chamber center to the ground monitoring points, the accumulated exploitation volume of extraction space, and the measured/recorded time. These four measurements were used as inputs for the ANN model to predict land subsidence.

The hyperparameters of the ANN model, including the number of hidden layers, hidden nodes, and iterated epochs, were determined by *k*-fold cross-validation. Subsequently, they were utilized to estimate the model's parameters by the training set and predict land subsidence for the test set. The "optimal" hyperparameters were found to be 5 hidden layers, 64 hidden nodes, and 240 iterated epochs. The proposed ANN model with "optimal" hyperparameters found in this study was demonstrated to be a good tool for underground mining-induced land subsidence. Both RMSE and MAE of the predicted land subsidence depended on the time separation between the last measured epoch and the predicted epoch. Within 2 months from the last measurement, RMSE/MAE were found at 22 and 13 mm for Epoch 10. These numbers increased to 31 and 20 mm for Epoch 11 (4 months from the last measurement), and 37 and 24 mm for Epoch 12 (6 months from the last measurement).

References

[1] Fan, S., Yan, J., & Sha, J. (2017). Innovation and economic growth in the mining industry: Evidence from China's listed companies. *Resources Policy*, (54), 25-42. https://doi.org/10.1016/j.resourpol.2017.08.007

[2] Fleming, D.A., & Measham, T.G. (2014). Local job multipliers of mining. *Resources Policy*, (41), 9-15. https://doi.org/10.1016/j.resourpol.2014.02.005

[3] Nguyen, B.N., Boruff, B., & Tonts, M. (2021). Looking through a crystal ball: Understanding the future of Vietnam's minerals and mining industry. *The Extractive Industries and Society*, 8(3), 100907. https://doi.org/10.1016/j.exis.2021.100907

[4] Nguyen, B.N., Boruff, B., & Tonts, M. (2017). Mining, development and well-being in Vietnam: A comparative analysis. *The Extractive Industries and Society*, 4(3), 564-575. https://doi.org/10.1016/j.exis.2017.05.009

[5] Nguyen, Q.N., Nguyen, V.H., Pham, T.P., & Chu, T.K.L. (2021). Current status of coal mining and some highlights in the 2030 development plan of coal industry in Vietnam. *Inżynieria Mineralna*, 1(2). https://doi.org/10.29227/IM-2021-02-34

[6] Dorband, I.I., Jakob, M., & Steckel, J.C. (2020). Unraveling the political economy of coal: Insights from Vietnam. *Energy Policy*, (147), 111860. https://doi.org/10.1016/j.enpol.2020.111860

[7] Mohsin, M., Zhu, Q., Naseem, S., Sarfraz, M., & Ivascu, L. (2021). Mining industry impact on environmental sustainability, economic growth, social interaction, and public health: An application of semi-quantitative mathematical approach. *Processes*, 9(6), 972. https://doi.org/10.3390/pr9060972

[8] Zhu, X., Guo, G., Zha, J., Chen, T., Fang, Q., & Yang, X. (2016). Surface dynamic subsidence prediction model of solid backfill mining. *Environmental Earth Sciences*, 75(12), 1007. https://doi.org/10.1007/s12665-016-5817-9

[9] Brady, B.H.G., & Brown, E.T. (2004). *Rock mechanics for underground mining*. Berlin, Germany: Springer Science + Business Media B.V., 628 p. https://doi.org/10.1007/978-1-4020-2116-9

[10] Marschalko, M., Yilmaz, I., Křístková, V., Fuka, M., Kubečka, K., Bouchal, T., & Bednarik, M. (2012). Optimization of building site category determination in an undermined area prior to and after exhausting coal seams. *International Journal of Rock Mechanics and Mining Sciences*, (54), 9-18. https://doi.org/10.1016/j.ijrmms.2012.05.021

[11] Todorović, R.T. (1993). Precise levelling network adjustment in mining subsidence regions. *Applications of Geodesy to Engineering*, 209-214. https://doi.org/10.1007/978-3-642-77958-9_19

[12] Jing-xiang, G., & Hong, H. (2009). Advanced GNSS technology of mining deformation monitoring. *Procedia Earth and Planetary Science*, 1(1), 1081-1088. https://doi.org/10.1016/j.proeps.2009.09.166

[13] Bian, H.-F., Zhang, S.-B., Zhang, Q.-Z., & Zheng, N.-S. (2014). Monitoring large-area mining subsidence by GNSS based on IGS stations. *Transactions of Nonferrous Metals Society of China*, 24(2), 514-519. https://doi.org/10.1016/S1003-6326(14)63090-9

[14] Bui, X.-N., Tran, V.A., Bui, L.K., Nguyen, Q.L., Le, T.T.H., & Ropesh, G. (2021). Mining-induced land subsidence detection by persistent scatterer InSAR and Sentinel-1: Application to Phugiao Quarries, Vietnam. *Proceedings of the International Conference on Innovations for Sustainable and Responsible Mining*, 18-38. https://doi.org/10.1007/978-3-030-60269-7_2

[15] Nguyen, Q.L., Tran, V.A., & Bui, L.K. (2021). Determination of ground subsidence by Sentinel-1 SAR data (2018-2020) over Binh Duong Quarries, Vietnam. *VNU Journal of Science: Earth and Environmental Sciences*, 37(2), 69-83. https://doi.org/10.25073/2588-1094/vnuees.4605

[16] Kim, T.T.H., Tran, H.H., Bui, L.K., & Lipecki, T. (2021). Mining-induced land subsidence detected by Sentinel-1 SAR images: An example from the historical Tadeusz Kościuszko Salt Mine at Wapno, Greater Poland Voivodeship, Poland. *Inzynieria Mineralna*, 48(2), 41-52. https://doi.org/10.29227/IM-2021-02-04

[17] Ma, C., Li, H., & Zhang, P. (2017). Subsidence prediction method of solid backfilling mining with different filling ratios under thick unconsolidated layers. *Arabian Journal of Geosciences*, 10(23), 511. https://doi.org/10.1007/s12517-017-3303-7

[18] Aston, T.R.C., Tammemagi, H.Y., & Poon, A.W. (1987). A review and evaluation of empirical and analytical subsidence prediction techniques. *Mining Science and Technology*, 5(1), 59-69. https://doi.org/10.1016/S0167-9031(87)90924-8

[19] Bahuguna, P.P., Srivastava, A.M.C., & Saxena, N.C. (1991). A critical review of mine subsidence prediction methods. *Mining Science and Technology*, 13(3), 369-382. https://doi.org/10.1016/0167-9031(91)90716-P

[20] Ambrožič, T., & Turk, G. (2003). Prediction of subsidence due to underground mining by artificial neural networks. *Computers & Geosciences*, 29(5), 627-637. https://doi.org/10.1016/S0098-3004(03)00044-X

[21] Lee, S., Park, I., & Choi, J.-K. (2012). Spatial prediction of ground subsidence susceptibility using an artificial neural network. *Environmental Management*, *49*(2), 347-358. https://doi.org/10.1007/s00267-011-9766-5

[22] Rafie, M., & Samimi Namin, F. (2015). Prediction of subsidence risk by FMEA using artificial neural network and fuzzy inference system. *International Journal of Mining Science and Technology*, *25*(4), 655-663. https://doi.org/10.1016/j.ijmst.2015.05.021

[23] Yang, W., & Xia, X. (2013). Prediction of mining subsidence under thin bedrocks and thick unconsolidated layers based on field measurement and artificial neural networks. *Computers & Geosciences*, (52), 199-203. https://doi.org/10.1016/j.cageo.2012.10.017

[24] Zou, J., Han, Y., & So, S.-S. (2009). Overview of artificial neural networks. *Artificial Neural Networks: Methods and Applications*, 14-22. https://doi.org/10.1007/978-1-60327-101-1_2

[25] Amari, S.-I. (1993). Backpropagation and stochastic gradient descent method. *Neurocomputing*, *5*(4), 185-196. https://doi.org/10.1016/0925-2312(93)90006-O

[26] Fushiki, T. (2011). Estimation of prediction error by using K-fold cross-validation. *Statistics and Computing*, *21*(2), 137-146. https://doi.org/10.1007/s11222-009-9153-8

[27] Chai, T., & Draxler, R.R. (2014). Root mean square error (RMSE) or mean absolute error (MAE)? – Arguments against avoiding RMSE in the literature. *Geoscientific Model Development*, *7*(3), 1247-1250. https://doi.org/10.5194/gmd-7-1247-2014

[28] Cort, J.W., & Kenji, M. (2005). Advantages of the mean absolute error (MAE) over the root mean square error (RMSE) in assessing average model performance. *Climate Research*, *30*(1), 79-82. https://doi.org/10.3354/cr030079

[29] Schmidt-Hieber, J. (2020). Nonparametric regression using deep neural networks with ReLU activation function. *The Annals of Statistics*, *48*(4), 1875-1897. https://doi.org/10.1214/19-AOS1875

[30] Han, J., & Moraga, C. (1995). The influence of the sigmoid function parameters on the speed of backpropagation learning. *From Natural to Artificial Neural Computation*, 195-201. https://doi.org/10.1007/3-540-59497-3_175

[31] Lau, M.M., & Lim, K.H. (2018). Review of adaptive activation function in deep neural network. *Proceedings of the IEEE-EMBS Conference on Biomedical Engineering and Sciences*, 18415201. https://doi.org/10.1109/IECBES.2018.8626714

[32] Buscema, M. (1998). Back propagation neural networks. *Substance Use & Misuse*, *33*(2), 233-270. https://doi.org/10.3109/10826089809115863

[33] Zou, F., Shen, L., Jie, Z., Zhang, W., & Liu, W. (2019). A sufficient condition for convergences of Adam and RMSProp. *Proceedings of the IEEE/CVF Conference on Computer Vision and Pattern Recognition*, 19263324. https://doi.org/10.1109/cvpr.2019.01138

[34] Raju, V.N.G., Lakshmi, K.P., Jain, V.M., Kalidindi, A., & Padma, V. (2020). Study the influence of normalization/transformation process on the accuracy of supervised classification. *Proceedings of the Third International Conference on Smart Systems and Inventive Technology*, 20032431. https://doi.org/10.1109/ICSSIT48917.2020.9214160

Прогнозування просідання, спричиненого підземними гірничими роботами: підхід на основі штучної нейронної мережі

Л.К. Нгуен, Т.Т.Т. Ле, Т.Г. Нгуен, Д.Т. Тран

Мета. Прогнозування просідання земної поверхні при підземному видобуванні вугілля на основі застосування штучної нейронної мережі (ШНМ) для ефективного управління земельними ресурсами та планування інфраструктури на прикладі шахти Монг Дуонг у Куанг Нінь, В'єтнам.

Методика. У моделі ШНМ, запропонованої у цьому дослідженні, чотири показники застосовуються як вхідні дані: положення наземних точок у напрямку основного поперечного перерізу жолоба, відстань від центру камери (виробленого простору) до наземних точок спостереження, накопичений експлуатаційний обсяг виїмкового простору та виміряний/зареєстрований час. Весь набір даних із 12 виміряних епох, що охоплюють 22 місяці з 2-місячним періодом повторення, розділено на навчальну вибірку для перших 9 виміряних епох та тестову вибірку для останніх 3 виміряних епох. k-кратна кросс-валідація спочатку застосовується до навчальної вибірки, щоб визначити найкращі гіперпараметри моделі, які потім приймаються для прогнозування просідання ґрунту у тестовій вибірці.

Результати. Виявлено, що найкращими гіперпараметрами моделі є 5 прихованих шарів, 64 приховані вузли та 240 ітерованих епох. Визначено, що середньоквадратична похибка (СКП) і середня абсолютна похибка (САП) прогнозованого просідання ґрунту залежать від часу, розділеного між останньою виміряною епохою та прогнозованою епохою. Протягом 2 місяців після останніх вимірювань СКП і САП становлять 22 і 13 мм для епохи 10, які збільшуються до 31 і 20 мм для епохи 11 (4 місяці з моменту останнього вимірювання) та 37 і 24 мм для епохи 12 (6 місяців з моменту останнього вимірювання).

Наукова новизна. У цьому дослідженні запропоновано нову модель ШНМ із відповідними "оптимальними" гіперпараметрами для прогнозування просідання ґрунту, спричиненого підземними гірничими роботами.

Практична значимість. Пропонована в даному дослідженні модель ШНМ є гарним та зручним інструментом для оцінки просідання ґрунту, спричиненого гірничими роботами, яка може бути застосована до підземних шахт у провінції Куанг Нінь, В'єтнам.

Ключові слова: прогнозування просідання, підземна шахта, машинне навчання, штучна нейронна мережа (ШНМ)